II International Conference on Particle-based Methods – Fundamentals and Applications
PARTICLES 2011
E. Oñate and D.R.J. Owen (Eds)

INFLUENCE OF IMPACT VELOCITY ON THE FRAGMENT FORMATION OF CONCRETE SPECIMENS

DIPL.-ING. STEVE WERNER*; PROF. DR.-ING. KARL-CHRISTIAN THIENEL*

*Institut für Werkstoffe des Bauwesens (IWB)
Universität der Bundeswehr München
Werner-Heisenberg-Weg 39, 85579 Neubiberg, Deutschland
e-mail: steve.werner@unibw.de, internet: http://www.unibw.de/bauv3

Key words: Impact velocity, Fragment analyzing, Fracture surface determination

Abstract. *In recent years some studies presented fragmentation models to describe the impact of projectiles [e. g.: 1, 2]. This paper shows results of high velocity impact of gun projectiles on concrete specimens. Three different muzzle velocities were tested on a standard concrete with special attention on the surface area generated. The penetration of the projectiles resulted in two craters (one on the front and one on the rear side of the specimens) and the formation of a huge number of particles of various shapes and sizes. The crater surfaces were analyzed with the 3-dimensional laser-scanner DAVID 3D which utilizes triangulation. The detailed principle is described in [3]. Parameters to describe the particles were determined with a CPA (camera particle analyzer). The used Haver CPA 2-1 is based on digital image processing with a high-resolution digital line scan camera. The following information were obtained: the shape-parameter sphericity, the particle-size-parameters (Feret-diameter, length, volume distribution) and the numbers of particles. A triaxial ellipsoid model was developed to determine the surface of the particles which takes a particle-shape-parameter into account. The main advantage of the ellipsoid model compared to the normally used sphere model is the consideration of the volume determined. The ellipsoid model provides a better picture of the real particle surfaces. Besides these sample related parameters the speed of the projectile was measured before and after penetrating the concrete specimens. As a result both kinetic energies could be calculated. Their difference corresponds to sum of the energy necessary to generate the fracture particles and their kinetic energy following the impact. In the course of this study a correlation was established between the energy difference (fracture energy + kinetic energy) and the fracture surface area generated. An increasing energy difference led to an increasing fracture surface area and higher number of particles as well. These results of the study can be utilized for designing protective concrete structures.*

1 INTRODUCTION

In recent years several studies dealt with the fragmentation of different materials like steel and ceramic due to projectile impact [2, 4, 5]. If a specimen is perforated by a projectile, energy is absorbed by the specimen respectively by creating fragments of different shape and size. These fragments form fragment clouds at the front and rear side of the specimen. An overview of a few studies, which investigated the formation and propagation of fragment clouds behind thin bumpers, can be found in [2]. These studies led to models describing the

fragment clouds and the dissipated energy, but most of them dealt with metallic materials only.

The knowledge about concrete is insufficient with respect to the formation of fragment clouds. Because of the complex effects observed in impact tests on concrete the evaluation of the results is often simplified; e.g. the damage of the concrete specimen is classified simply in perforated or non perforated [6]. Other studies are more focused on the penetration depth to measure local damage. More information can be found in [7]. Nevertheless these simplified descriptions were subsequently used to determine all kinds of influences, e.g. water/cement - ratio [7, 8, 9]. The fragments were never considered.

Thus, one of the aims of this study is to analyze concrete fragments resulting from an impact perforation. A camera particle analyzer (CPA) was used for this purpose. This technique is commonly applied to sand, coal, glass, food etc. [e. g. 10, 11, 12]. Once the distribution and the shape of the fragments are known, the damage of the specimens can be described as a function of the newly created surface area. Additionally, the crater surface left in the specimens must be measured, too. This was done using a 3D laser-scanner.

Due to projectile impact a part of the kinetic energy of the projectile is converted into fracture energy creating fragments. *Dinovitzer* [1] divided the energy into "target plug fracture energy, projectile impact kinetic energy, target debris kinetic energy, residual penetrator kinetic energy and deformation and heat energy loss". *Schäfer* [2] combined the thermally and mechanically dissipated energy and called them "dissipated" energy. In this paper the energy is only divided into the kinetic energy of the projectile and the energy difference ΔE which includes the fragment energy and kinetic energy of the fragments. The main focus was the correlation between the energy difference and the muzzle velocities of the projectiles.

2 EXPERIMENTAL INVESTIGATION

2.1 Concrete mixture and properties

A normal strength concrete mix was chosen to compare the impact effect of munition with different muzzle velocities on specimens. Details of the mix design of the concrete are given in Table 1.

Table 1: Mix design

w / c [-]	Water [kg/m^3]	Cement [kg/m^3]	Sand 0 / 4 [kg/m^3]	Gravel 4 / 8 [kg/m^3]	Gravel 8 / 16 [kg/m^3]
0.6	185	310	847	364	680

The binder was a German CEM I Portland cement with a minimum strength of 42.5 N/mm^2 at an age of 28 days. The ratio between water and cement was 0.60. Aggregate was a limestone from a local quarry with a maximum grain size of 16 mm. For each velocity tested ten specimens were cast. The specimens were demoulded after one day and subsequently stored in lime-saturated water for 27 days until testing.

The mechanical properties were measured at 28 days. Compressive strength and Young´s modulus were determined in each case on three cylindrical specimens (d / h = 150 / 300 mm) according to [13]. Three beams (l / w / h = 100 / 100 / 500 mm) were used in each case to determine the bending tension strength according to [13]. The mean values of all specimens and their coefficents of variation are presented in Table 2.

Table 2: Mechanical properties (in parentheses: coefficient of variation)

ρ [kg / dm^3]	f_c [MPa]	E [GPa]	f_{ft} [MPa]
2.475 (0.002)	48.42 (0.016)	32.1 (0.011)	6.81 (0.037)

2.2 Impact investigation

The concrete specimens had a quadratic size of 30 x 30 cm^2 and a thickness of 5 cm only. Thus, edge effects could be minimized and a perforation of the specimens due to the projectile impact was ensured. The munitions were jacketed projectiles with a hard core of tungsten carbide. Each projectile has a length of 51 mm and a diameter of 7.62 mm with a weight of 9.5 g. These projectiles are used as special munitions of the German army for the rifle HK G3.

The tests were conducted in the ballistic laboratory at the Universität der Bundeswehr München, where different ballistic test conditions could be examined. In this study the tests were carried out with a measuring weapon system (MWS) of Mauser. One advantage of this MWS is the ability to vary the muzzle velocity. The specimens were installed in a steel frame inside a backstop (L / W / H = 2.0 / 0.7 / 0.7 m) of 8 mm thick steel. The distance between the MWS and the backstop was 13 m. To determine the speed of the projectiles two photoelectric barriers were placed between the MWS and the backstop; one in front of the MWS (muzzle velocity) and the second close to the backstop (impact velocity). After perforation the speed of the projectile was determined with a double exposed picture of a digital camera (Figure 1), which is placed behind a PMMA window at one side of the backstop. The speed could be calculated from the time difference of two flashes (here: 0.1 ms) and the distance of the projectile within this time difference using the double exposed picture.

Based on the measured speed of the projectile and its known weight the kinetic energy before and after perforation could be calculated. Their difference corresponds to the energy necessary to generate the fracture particles and their kinetic energy following the impact.

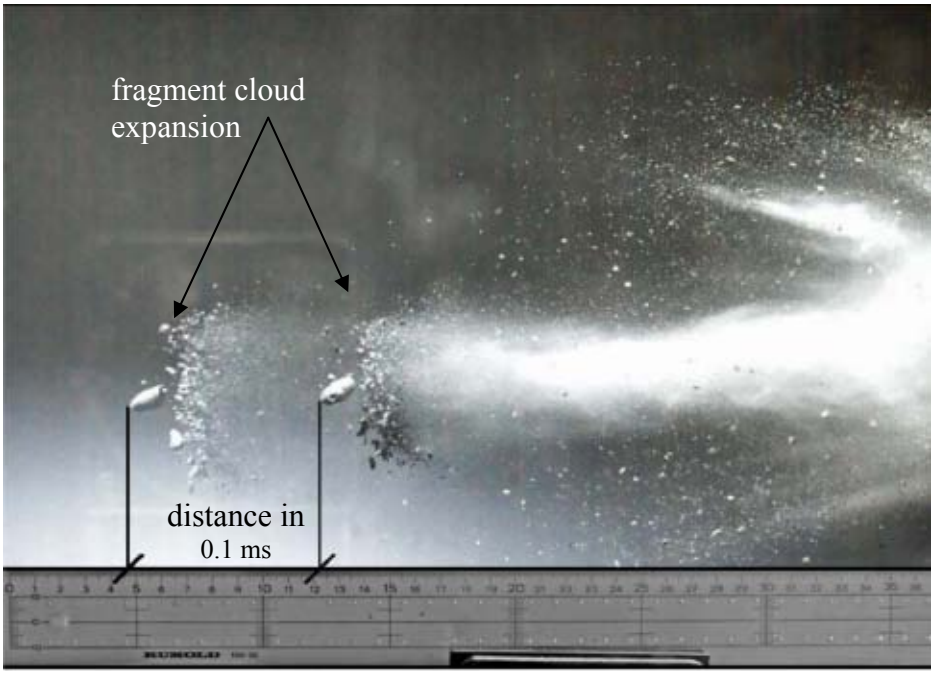

Figure 1: Double exposed picture of a projectile after perforation

2.3 Surface determination

As a consequence of the perforation a fractured surface area was created which consists of different parts. One part consists of the crater-area on the front and rear side of the specimen. The laser scanning system DAVID 3D was used to determine these surfaces. It is based on laser triangulation [3]. The setup of the laser scanning system consists of a line laser, a digital video camera (here a Sony DigiCam), a 90 °-corner with a calibration pattern and the software DAVID. The principle arrangement of the measuring setup is given in Figure 2.

The line laser was installed in a small lift in order to assure reproducible test conditions. Thus, the laser went up and down and the intensity of the different scans was almost constant. The laser plane of the line laser intersects with the calibration pattern in the corner. In this study the calibration point distance for the camera was 300 mm and the surface smoothing operators for scanning and processing were used according to the recommendation of the manufacturer: interpolate = 4, smooth average = 2, and smooth median = 0. The new 3-dimensional coordinates of a single point are calculated by means of optical triangulation. As a result, the points scanned form a 3-dimensional point cloud defining the surface area, which then in turn can be calculated.

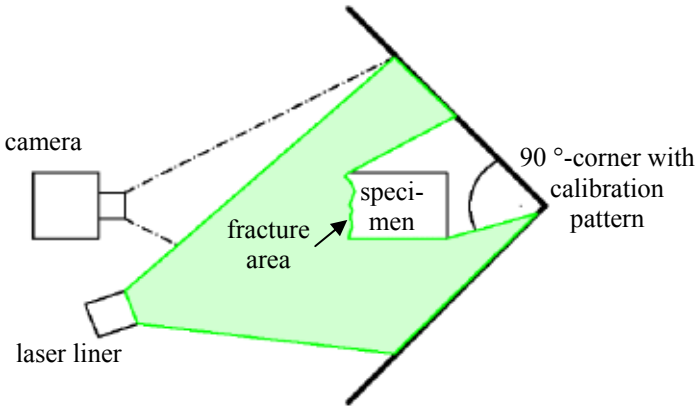

Figure 2: Measurement setup for the contact-free scanning of 3-dimensional objects with DAVID 3D

The second part of the fractured surface area is provided by the fragments which were disrupted from the specimens as a result of the projectile impact. Their surface area was determined using a computer particle analyzer (CPA) of Haver & Boker [14]. The CPA is based on digital image processing with a high-resolution digital line scan camera. It measures the shape-parameter sphericity, particle-size-parameters (Feret-diameter, length, volume distribution) and particle numbers of each size class analogue to a sieving analysis (following the sieving sequence R 20/3 of [15]).

A mathematical model is necessary to describe the surface area of the fragments. A sphere model was discarded for this purpose because the calculated volume of the particles as sphere was nearly two times higher than the measured volume (with: sphere-diameter = Feret-diameter). Thus, a triaxial ellipsoid model was chosen to determine the surface of the particles. By knowing two of three half axes of an ellipsoid (average Feret-diameter and average length of each size class) the third axis could be calculated by using the known volume V. The formula of *Thomsen* [16] for the surface area of the ellipsoid led to a good approximation. Additionally, a shape factor was developed which considered the particle-shape-parameter measured. The shape factor is defined as the quotient of the measured sphericity Circ and the sphericity $Circ_E$ of an ellipse constructed of the measured Feret-diameter F and the length L. The surface area of each size class A_{SC} could be calculated by equation (1) where N_{SC} means the number of particles of this size class.

$$A_{SC} = N_{SC} \cdot \frac{Circ}{Circ_E} \cdot 4 \cdot \pi \cdot \left(\frac{(F \cdot L)^{1,6} + \left(\frac{3 \cdot V}{N_{SC} \cdot 4 \cdot \pi \cdot F}\right)^{1,6} + \left(\frac{3 \cdot V}{N_{SC} \cdot 4 \cdot \pi \cdot L}\right)^{1,6}}{3} \right)^{0,625} \quad (1)$$

A part of the fragments surface was not created by the impact but comprises the original surface of the formwork. This part must be discounted from the total fragments surface in order to obtain the surface fractured only. Therefore, pictures of the front and rear side of the specimens were taken directly after the tests with a main focus on the crater. The software AutoCAD scaled these pictures to the needed size. Subsequently a polygon was drawn

enclosing the crater. The resulting area enclosed by the polygon represented the original surface of the fragments before impact.

The fractured surface area comprises the sum of all surfaces of each size class plus the surface of the craters minus the original surface of the specimens.

3 EXPERIMENTAL RESULTS

3.1 Masses

The mean weight of the specimens before impact m_{bp} was measured to approx. 11200 g. After perforation the weight of the specimens m_{ap} decreased differently dependent of the weight of the detached fragments m_f. All masses are given in Table 3.

Table 3: Masses (in parentheses: coefficient of variation)

Test series	m_{bp} [g]	m_{ap} [g]	m_f [g]
875 m/s	11183 (0.010)	10830 (0.014)	327 (0.288)
710 m/s	11121 (0.015)	10864 (0.014)	237 (0.256)
605 m/s	11199 (0.026)	10955 (0.027)	228 (0.267)

3.2 Velocity and energy

The mean values of the measured velocities and the energy difference calculated are given in Table 4. The energy differences were calculated using the velocities before and after impact and assuming a constant mass of the projectile (9.5 g). In most cases the tungsten carbide core was not destroyed; thus, no energy was used for deforming the core. The energy differences rise with an increasing muzzle respectively impact velocity.

Table 4: Mean velocities measured (in parentheses: coefficient of variation)

Test series	v_{impact} [m/s]	$v_{after\ perforation}$ [m/s]	ΔE [J]
875 m/s	875.7 (0.005)	664.8 (0.054)	1538 (0.135)
710 m/s	710.3 (0.005)	484.5 (0.049)	1279 (0.087)
605 m/s	605.2 (0.005)	348.9 (0.103)	1156 (0.098)

3.3 Number of fragments and surface area

The number of fragments increases with a higher muzzle velocity and a smaller sieving width. Figure 3 shows the mean numbers of fragments of all test series dependent of their size. The diagram has a bi-logarithmic scale. The highest number of fragments during testing all three velocities can be found in the sieving class 0.125 / 0.18 mm. The sum of all

fragments varied between 1.94 million for 605 m/s and 4.17 million for 875 m/s. For a speed of 710 m/s 2.66 million fragments were measured.

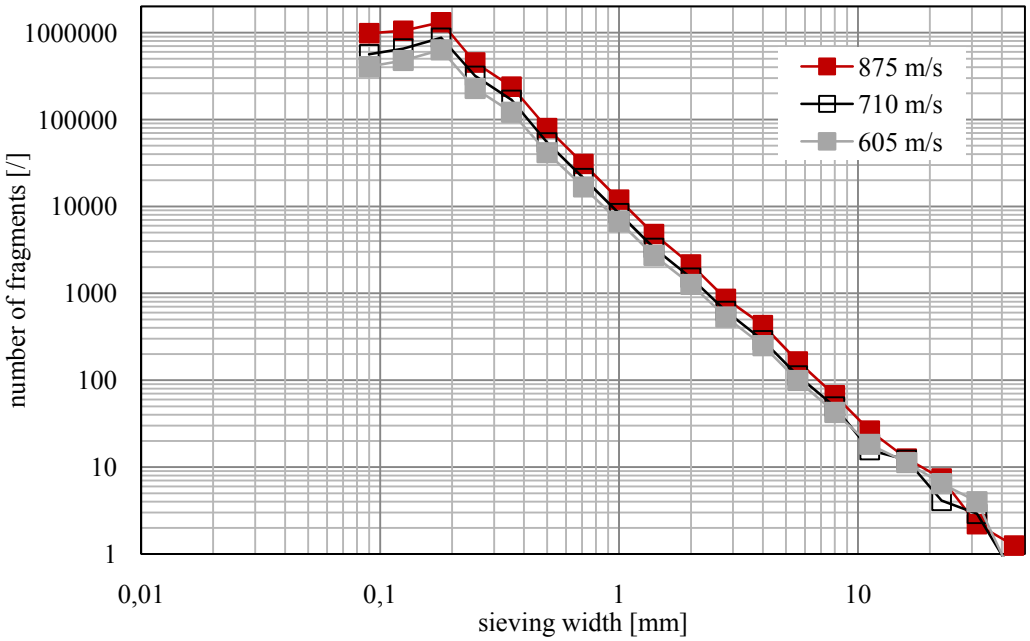

Figure 3: Number of fragments in different sieving classes

The mean values of the sphericity of the fragments were in the same range irrespective of the impact speed. They vary between 1.21 (710 m/s) to 1.25 (605 m/s) and 1.26 (875 m/s).

The surface areas of the fragments were calculated from the values measured with the CPA. These surfaces are considerably greater than the corresponding crater surfaces. The mean sum of the surface areas of the front and the rear of each specimen detected with the laser-scanner was significantly higher for the highest muzzle velocity, but for the two other velocities the crater areas are more or less the same. All mean values and their coefficent of variation are presented in Table 5.

Table 5: Surface areas (in parentheses: coefficient of variation)

Test series	A_{crater} [cm^2]	$A_{fragments}$ [cm^2]	$A_{original}$ [cm^2]	$A_{fractured\ area}$ [cm^2]
875 m/s	213 (0.178)	4836 (0.085)	194 (0.274)	4855 (0.877)
710 m/s	166 (0.193)	3187 (0.117)	146 (0.200)	3207 (0.118)
605 m/s	167 (0.205)	2656 (0.109)	149 (0.195)	2674 (0.110)

4 DISCUSSION

The combined masses after perforation are marginally smaller than the masses before testing. The differences are about 0.2 % of the initial weights (but around 10 % of the

fragments weights). It can be assumed that all bigger fragments were found and measured. Thus, the loss of weight can be considered a loss of the finest fragments. This assumption is supported by the distribution of the number of particles (Figure 3). It could be expected that the number of fragments increases with a smaller sieving width, but it decreases for the finest measured sizes (< 0.8 mm). As a result the surface areas calculated are too small. This could be disregarded as long as different velocities are compared due to the fact that these mass losses occur in each of the test series.

The fractured surface area increases with a higher impact velocity, but a detailed analysis of different parts of it reveals a more complex situation. On one hand the area of the crater is almost equal for impact velocities of 605 m/s and 710 m/s while it differs for an impact velocity of 875 m/s. On the other hand the fragment area increases significantly with an increasing impact velocity as a result of the higher number of fragments, especially finer ones, created during the impact perforation. This situation shows the importance of a detailed fragment analysis. A simple measurement and evaluation of the crater surfaces only as it was done in earlier studies would result in misleading conclusions about the damage caused by impact.

As expected the energy of the projectile before and after perforating the specimens increases with the rising impact velocity. The interesting point is that the energy differences also increase with rising impact velocities. It is assumed that the energy difference consists of fracture energy to create fractured surface areas and kinetic energy to project the fragments out of the specimens. Thus, higher energy differences stand for more fracture energy and / or more kinetic energy of the fragments. The double exposed pictures show besides the projectile the maximum expansion of the fragment cloud. It reached almost the same speed as the projectile at that time. As a consequence the kinetic energy of the fragments increases with a higher impact velocity due to their higher speed and simultaneously their rise of masses. The higher fragment masses correspond with higher fracture areas. In order to create these areas more energy is consumed. Thus, the fracture energy increases also with higher impact velocities. This assumption is supported by fracture mechanical tests. Different studies show a rise of fracture energy when tested at higher speeds [17, 18, 19, 20]. One reason for this correlation could be seen in a higher strength and a higher deformability, but the exact explanation is not yet found.

Figure 4 shows the fracture surface areas and energy differences. The figure includes the mean values together with the minimum and maximum values of all test series. The Figure summarizes the question of this study: Does a higher muzzle velocity cause higher energy differences and an increased fracture surface area?

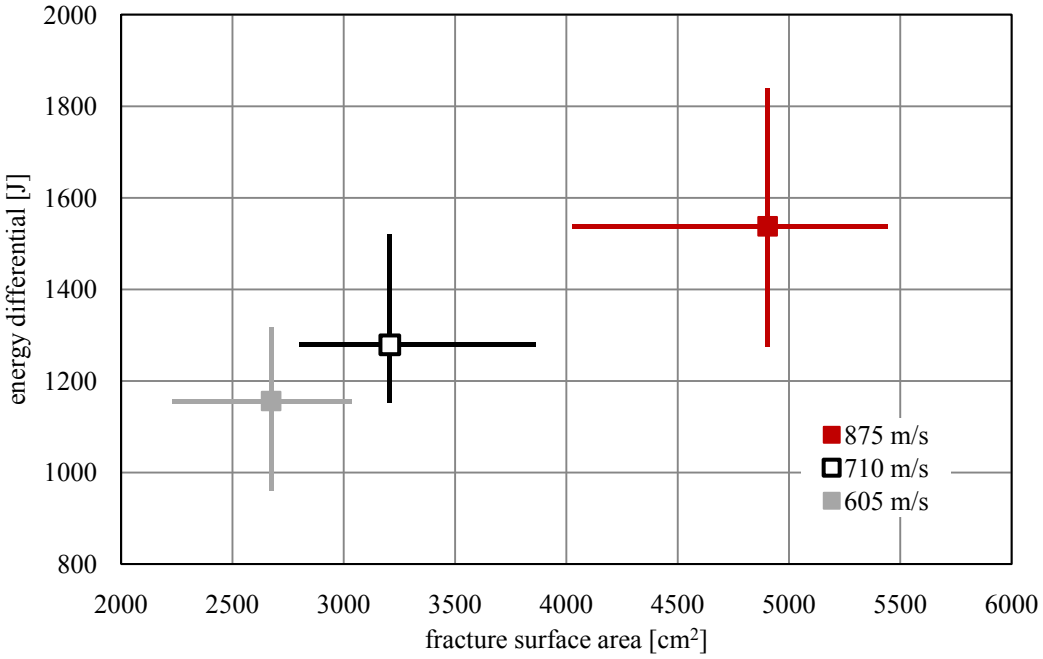

Figure 4: Linear connection of the fractured surface area and the energy differentials

5 CONCLUSION AND OUTLOOK

In this study the damage on concrete specimen due to different impact velocities of projectiles were determined with special focus on the fracture surface area created. The marginal differences of the crater areas show that this criterion is insufficient to describe the damage. A thorough investigation must be based on measurements of all parts of the fractured area. Therefore a detailed fragment analysis is necessary. The largest part of the fracture area is provided by the surface of the fragments. These fragments are created by energy transformation. The kinetic energy of the projectile changed partial into fracture energy and kinetic energy of the fragments.

The two main conclusions of this paper are:

- Higher impact velocities lead to higher energy differences; thus, more kinetic energy of the projectile is absorbed and
- Higher impact velocities lead to higher fractured surface areas and hence a larger damage.

This knowledge can be used for designing concrete structures against impact. Future work will focus on different influences of concrete mix design upon impact perforation. Besides this, the energy parts within the energy differences have to be determined more closely.

REFERENCES

[1] Dinovitzer, A. Fragmentation of targets during ballistic penetration events. *Int. J. Imp. Eng*. (1998) **21**:237–244.

[2] Schäfer, F. An engineering fragmentation model for the impact of spherical projectiles on thin metallic plates. *Int. J. Imp. Eng* (2006) **33**:745–762.
[3] Winkelbach, S., Molkenstruck, S. and Wahl, F. Low-Cost Laser Range Scanner and Fast Surface Registration Approach, in: Pattern recognition. 28th DAGM Symposium, Berlin, Germany, September 12 - 14, 2006 (Franke, K., Müller, K.-R., Nickolay, B. and Schäfer, R., Ed), pp. 718–728. Springer, Berlin.
[4] Dean, J., Dunleavy, C., Brown, P. and Clyne, T. Energy absorption during projectile perforation of thin steel plates and the kinetic energy of ejected fragments. *Int. J. Imp. Eng* (2009) **36**:1250–1258.
[5] Grady, D. Fragment size distributions from the dynamic fragmentation of brittle solids. *Int. J. Imp. Eng* (2008) **35**:1557–1562.
[6] Dancygier, A.N. and Yankelevsky, D.Z. Effects of Reinforced Concrete Properties on Resistance to Hard Projectile Impact. *ACI Str. J.* (1999) **96**:259–267.
[7] Vossoughi, F., Ostertag, C., Monteiro, P. and Johnson, G. Resistance of concrete protected by fabric to projectile impact. *Cem. Con. Res.* (2007) **37**:96–106.
[8] Bludau, C. Schutzplatten aus hochfestem Beton. *Berichte des konstruktiven Ingenieurbaus* (2006) Inst. für Mechanik und Statik Univ. der Bundeswehr München. Neubiberg.
[9] Kustermann, A., Zimbelmann, R.K., Keuser, M. and Grimm, R. Hochfeste Bindemittel und Zuschlagstoffe für hochfeste Betone unterschiedlicher Güte für Schutzanlagen der militärischen Sonderinfrastruktur (2001) Neubiberg.
[10] Breitenbücher, R. Online-Messung der Korngrößenverteilung von Sand. *Beton* (2005) **55**:436–443.
[11] Zlatev, M. Beitrag zur quantitativen Kornformcharakterisierung unter besonderer Berücksichtigung der digitalen Bildaufnahmetechnik (2005). Niedersächsische Staats- und Universitätsbibliothek. Göttingen, Freiberg (Sachsen).
[12] Hodenberg, M.F. von Optimierung der Kies- und Sandgewinnung auf einem Baggerschiff durch vollautomatische Online-Korngrößenanalyse. *Aufbereitungstechnik (at mineral processing)* (2000) **41**:561–566.
[13] Deutsches Institut für Normung Prüfung von Festbeton DIN EN 12390 (2009). Beuth.
[14] Haver&Boker Haver CPA-Messprinzip.
http://www.weavingideas.com/de/anwendungen-produkte/partikelanalyse-photooptisch/mehr-ueber-haver-cpa/cpa-messprinzip.html. (last call: 5.5.11)
[15] Deutsches Institut für Normung Analysensiebe. Metalldrahtgewebe, Lochplatten und elektrogeformte Siebfolien : Nennöffnungsweiten : DIN ISO 565 (1998). Beuth.
[16] Michon, G.P. Final answers. Surface Area of an Ellipsoid.
http://www.numericana.com/answer/ellipsoid.htm. (last call: 5.5.11)
[17] Brara, A. and Klepaczko, J. Fracture energy of concrete at high loading rates in tension. *Int. J. Imp. Eng* (2007) **34**:424–435.
[18] Vegt, I., Weerheijm, J. and van Breugel, K. The rate dependency of concrete under tensile impact loading. Fracture energy and fracture characteristics. (2009) *proceedings, 13th Int. Symp. Interaction effects munitions with structures (ISIMS)*
[19] Zhang, X., Ruiz, G., Yu, R. and Tarifa, M. Fracture behaviour of high-strength concrete at a wide range of loading rates. *Int. J. Imp. Eng* (2009) **36**:1204–1209.

[20] Schuler, H., Mayrhofer, C. and Thoma, K. Spall experiments for the measurement of the tensile strength and fracture energy of concrete at high strain rates. *Int. J. Imp. Eng* (2006) **32**:1635–1650.